Molecular determinants for CC-chemokine recognition by a poxvirus CC-chemokine inhibitor

Bruce T. Seet*†, Rajkumari Singh†, Chad Paavola‡, Elaine K. Lau‡, Tracy M. Handel‡, and Grant McFadden*†§

*Viral Immunology & Pathogenesis Laboratories, John P. Robarts Research Institute, 1400 Western Road, Room 133, London, ON, Canada N6G 2V4; †Department of Microbiology and Immunology, University of Western Ontario, London, ON, Canada N6A 5C1; and ‡Department of Molecular and Cell Biology, University of California at Berkeley, Berkeley, CA 94720

Edited by Bernard Moss, National Institutes of Health, Bethesda, MD, and approved June 15, 2001 (received for review February 11, 2001)

Poxviruses express a family of secreted proteins that bind with high affinity to chemokines and antagonize the interaction with their cognate G protein-coupled receptors (GPCRs). These viral inhibitors are novel in structure and, unlike cellular chemokine receptors, are able to specifically interact with most, if not all, CC-chemokines. We therefore sought to define the structural features of CC-chemokines that facilitate this broad-spectrum interaction. Here, we identify the residues present on human monocyte chemoattractant protein-1 (MCP-1) that are required for high-affinity interaction with the vaccinia virus 35-kDa CC-chemokine binding protein (VV-35kDa). Not only do these residues correspond to those required for interaction with the cognate receptor CCR2b but they are also conserved among many CC-chemokines. Thus, the results provide a structural basis for the ability of VV-35kDa to promiscuously recognize CC-chemokines and block binding to their receptors.

CCR2b | chemokine binding protein | monocyte chemoattractant protein-1 | mutagenesis | surface plasmon resonance

The directed migration of leukocytes into areas of inflammation or infection is an integral feature of the immune response. This process is coordinated by chemokines, a class of chemotactic cytokines that are secreted in response to a wide variety of inflammatory stimuli (1–3). Chemokines are divided into four families based on the pattern of cysteine residues (C, CC, CXC, and CX_3C), and they exert their effects by binding and signaling through seven transmembrane G protein-coupled receptors (GPCRs) on the surface of leukocytes. Although the molecular details remain unclear, mutagenesis and NMR studies have revealed some of the structural requirements for receptor binding and activation (4–15). Collectively, these studies support a hypothesis whereby chemokines activate their receptor through a putative two-step mechanism. One important feature of the interaction involves epitopes scattered on the face of chemokine opposite the C-terminal helix, and contacts between this face and the N terminus of the receptor (6, 7, 11, 14–18). A second interaction is mediated by the disordered N-terminal region of chemokines preceding the first disulfide motif, which has been shown to be necessary for receptor activation (5, 6, 8, 9, 12, 14, 15, 19–22).

Given that chemokines are so crucial to the host immune response, it is not surprising that viruses have evolved several strategies to manipulate or interfere with chemokine function (23–25). Poxviruses express a family of secreted proteins collectively known as the T1/35kDa CC-chemokine-binding proteins (CBPs) (26). These CBPs, which include the leporipoxvirus T1 and the orthopoxvirus 35-kDa proteins, bind with high affinity to many CC-chemokines from different species and competitively inhibit their interaction with their cellular receptors (26–30). Perhaps the most remarkable characteristic of these poxvirus CBPs is that they bear no resemblance to any known chemokine receptor or GPCR and that they have no known mammalian homologues. Whereas the crystal structure of the cowpox virus p35 CC-chemokine binding protein (CPV-p35) was recently determined (31), the manner in which this family of proteins is capable of promiscuously interacting with CC-chemokines remains unknown. Given their broad-spectrum ability to interact with so many CC-chemokines, we hypothesize that these poxvirus chemokine inhibitors recognize common structural features shared by most CC-chemokines.

In an effort to better understand the molecular nature of these interactions, we sought to identify epitopes on the surface of a CC-chemokine, monocyte chemoattractant protein-1 (MCP-1), that contribute to the binding to the VV-35kDa (vaccinia virus 35-kDa protein) CC-chemokine binding protein. Using a panel of deletion and site-directed MCP-1 mutants (6, 8, 32), we identified several residues that contribute to the high affinity interaction with VV-35kDa. Because these mutants were previously screened against CCR2b, it was also possible to compare the regions of MCP-1 that are involved in binding the viral inhibitor vs. the host receptor. This study reveals that VV-35kDa recognizes similar epitopes on MCP-1 that are important for binding to and signaling through CCR2b, demonstrating the use of common determinants by structurally distinct proteins.

Materials and Methods

Preparation and Characterization of Human MCP-1 Mutants. MCP-1 mutants were generated as described (6, 8, 32). All mutants were made in the context of MCP-1 M64I, which has been shown to behave identically to wild-type in binding assays to CCR2b. Kinetic parameters of wild-type MCP-1 (wtMCP-1) and M64I with respect to binding VV-35kDa are indistinguishable (data not shown). Mutants that had a large impact on binding to CCR2b (T10E, R24A, K49A, K35A, 34P35, and Y13A) were previously analyzed by NMR to verify that effects on binding were directly due to the mutation rather than indirect effects of structural perturbations (6).

Expression and Purification of Baculovirus-Expressed VV-35kDa Protein. VV-35kDa was expressed in a recombinant baculovirus system. Briefly, plasmid pCMVVL35-2 containing the gene encoding the vaccinia virus (strain Lister) 35kDa CC-chemokine binding protein was digested with *Bam*HI, and the fragment was inserted into *Bam*HI-digested pBacPAK1 (CLONTECH). To generate the recombinant virus, *Spodoptera frugiperda* (Sf-21) insect cells were cotransfected with *Bsu*36I-digested BacPAK6 viral DNA and pBacPACV-35K, following manufacturer's instructions (CLONTECH). To generate baculovirus-expressed VV-35kDa, Sf-21 cells grown in SF-900 serum-free medium (GIBCO/BRL) were infected with recombinant baculovirus expressing VV-35kDa. Supernatants from baculovirus-infected

This paper was submitted directly (Track II) to the PNAS office.

Abbreviations: CBP, chemokine binding protein; CPV, cowpox virus; GPCR, G protein-coupled receptor; MCP-1, monocyte chemoattractant protein-1; RU, response units; VV-35kDa, vaccinia virus 35-kDa protein; SPR, surface plasmon resonance; wt, wild type; MIP-1α, macrophage inflammatory protein-1α.

§To whom reprint requests should be addressed. E-mail: mcfadden@rri.on.ca.

The publication costs of this article were defrayed in part by page charge payment. This article must therefore be hereby marked "*advertisement*" in accordance with 18 U.S.C. §1734 solely to indicate this fact.

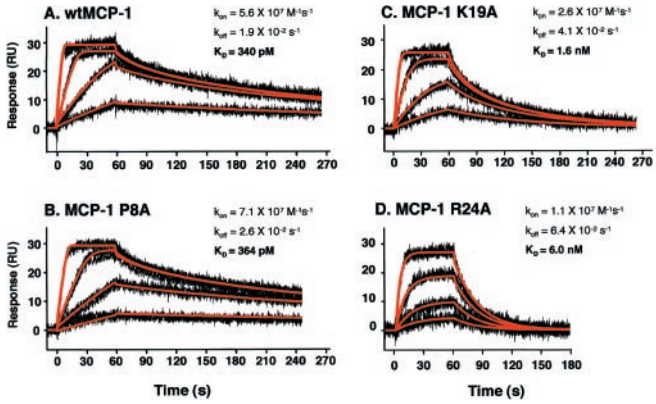

Fig. 1. Real-time binding data of wt and mutant human MCP-1 to the immobilized VV-35kDa protein. Sensorgrams are plotted as the mass of protein binding to immobilized VV-35kDa protein (in RU) as a function of time. Experimentally derived curves (black lines) from three repeat injections of (*A*) wtMCP-1 (*B*) MCP-1 P8A, (*C*) MCP-1 K19A, and (*D*) MCP-1 R24A at various concentrations are shown overlaid. Triplicate curves were globally fit with BIAEVALUATION 3.1 software using a 1:1 mass transport model (red lines) to determine the kinetic parameters presented in Table 1.

cells containing VV-35kDa were harvested 2 days postinfection and subjected to two rounds of anion exchange chromatography followed by size exclusion chromatography (HitrapQ, MonoQ, Superdex200 10/60; Amersham Pharmacia). Fractions were pooled, concentrated, and found to be >95% pure by silver-stained SDS/PAGE. To assess the molecular mass and oligomeric state of the baculovirus-expressed VV-35kDa protein, VV-35kDa was also subjected to a calibrated Superdex 200 16/60 size exclusion column.

Biomolecular Interaction Analysis Using Surface Plasmon Resonance (SPR). VV-35kDa was immobilized by using standard amine-coupling chemistry (33) to a level of ≈300 response units (RU; 300 pg/mm^2) onto a CM5 chip using a BIAcoreX biosensor (BIAcore, Uppsala). VV-35kDa-Fc fusion protein (R&D Systems) was immobilized via amine-coupled protein A. Chemokines were serially diluted in running buffer HBS-EP [10 mM Hepes, pH 7.4/150 mM NaCl/3 mM EDTA/0.005% polysorbate 20 (vol/vol)]. For association phases, 100 μl of chemokine was injected at a fast flow rate (100 μl/min) over both flow cells, and dissociation phases were monitored for up to 200 s by injecting HBS-EP. Surface regeneration was achieved by using 10 mM acetate, pH 4.0. Sensorgram deviations introduced by system noise were removed by using a second referencing sensorgram made from a 100-μl HBS-EP injection (34, 35). Data were globally analyzed with the analysis software BIAEVALUATION 3.0 (BIAcore) using a 1:1 mass transport model. Three sets of sensorgrams of four different concentrations (typically 0.93, 2.8, 8.3, and 25 nM) were each fit independently, and k_{on} and k_{off} were determined for each set. The equilibrium dissociation constant was determined by using the relationship between the mean values for k_{on} and k_{off} ($K_D = k_{off}/k_{on}$). To demonstrate reproducibility, sensorgrams of four concentrations of wild-type or mutant MCP-1, each performed in triplicate, were overlaid (Fig. 1). As a general criterion to assess the relative contribution of the mutations on binding of MCP-1, the difference in Gibb's free energy was determined ($\Delta\Delta G = RT \ln(K_{D(mut)}/K_{D(wt)})$, where R is the gas constant and T is 298 K). Single alanine mutations that resulted in a $\Delta\Delta G$ that exceeded 0.5 kcal·mol^{-1} were considered contact points that contribute to the interaction.

Stoichiometry of MCP-1 binding the VV-35kDa-Fc was assessed by using the following equation: $R_{max} = M_{r(MCP\text{-}1)}/M_{r(VV\text{-}35kDa\text{-}Fc)} \times RU_{(VV\text{-}35kDa\text{-}Fc\ bound)} \times$ valency. R_{max} is the mass of bound MCP-1 (in RU) at saturation, $M_{r(MCP\text{-}1)}$ and $M_{r(VV\text{-}35kDa\text{-}Fc)}$ are the relative molecular masses of monomeric MCP-1 (8000) and dimeric VV-35kDa-Fc protein (114,000), respectively, and $RU_{(VV\text{-}35kDa\text{-}Fc\ bound)}$ is the amount of immobilized VV-35kDa-Fc protein (200 RU).

Results

Surface Plasmon Resonance Demonstrates That Wild-Type MCP-1 Binds VV-35kDa with Picomolar Affinity. The CPV-p35 CC-chemokine inhibitor crystallized as a homodimer, in contrast to observations that suggested it exists as a monomer in solution (31). To determine the oligomeric state of baculovirus-expressed VV-35kDa, size exclusion chromatography demonstrated that the protein behaves as a homogeneous monomer with a molecular mass of ≈27 kDa (theoretical M_r of VV-35kDa is 27,828), whereas SDS/PAGE showed VV-35kDa migrating to 31 kDa (not shown). The smaller size of baculovirus-expressed VV-35kDa compared with the protein expressed in mammalian cells (35–40 kDa) reflects a lower level of glycosylation in insect cells as determined by glycosidase treatments (not shown).

Binding studies using VV-35kDa and other members of the T1/35kDa family of proteins with CC-chemokines demonstrated affinities in the low picomolar to nanomolar range (27–29). Using SPR, we determined that wild-type human MCP-1 binds VV-35kDa with rapid association kinetics ($k_{on} = 5.6 \times 10^7$ M^{-1}·s^{-1}) and reasonably slow dissociation kinetics ($k_{off} = 1.9 \times 10^{-2}$ s^{-1}), yielding a calculated K_D of 339 pM (Fig. 1*A*). This K_D was used as the reference for all MCP-1 mutants, which had affinity constants ranging from 143 pM to no discernible binding (Table 1, Fig. 2).

To assess potential steric effects caused by direct immobilization of VV-35kDa to the CM5 chip, VV-35kDa-Fc fusion protein was noncovalently immobilized to protein A on a CM5 chip (not shown). Kinetic analysis demonstrated that the VV-35kDa-Fc protein interacts with wtMCP-1 with an association rate and dissociation rate of 1.33×10^7 M^{-1}·s^{-1} and 1.72×10^{-2} s^{-1}, respectively. The resulting K_D of 1.29 nM is a result of a 4-fold slower k_{on} compared with VV-35kDa whereas k_{off} is similar for both proteins. The absence of any dramatic difference in binding MCP-1 by the two forms of the viral protein suggests that there are no severe effects caused by directly immobilizing VV-35kDa.

VV-35kDa Protein Monomer Binds Monomeric MCP-1. Many chemokines form homodimers or oligomers at high nanomolar to micromolar concentrations (36–39) whereas others exist strictly as monomers (40–44). For IL-8, MCP-1, MCP-2, and I-309, the monomeric form predominates in solution at physiological (nM) concentrations (32, 44, 45). Furthermore, several studies have shown that monomeric variants of chemokines are able to efficiently bind and activate their host receptors, suggesting that the monomer is the physiologically relevant form with respect to chemotaxis (32, 41, 46, 47). Among these studies, it was shown that an obligate monomeric variant of MCP-1 containing a mutation of proline at position 8 to alanine (P8A) induces chemotaxis of monocytes as potently as wtMCP-1 (32). We exploited this mutant to investigate whether MCP-1 binds VV-35kDa as a monomer or dimer. BIAcore sensorgrams generated with immobilized VV-35kDa protein binding wtMCP-1 or P8A showed that the binding kinetics and affinity constant of these two proteins are very similar (Fig. 1 *A* and *B*, Table 1). Importantly, MCP-1 P8A saturated at a R_{max} level identical to that of wtMCP-1, demonstrating that the monomeric form of MCP-1 interacts with VV-35kDa. Given that monomeric VV-35kDa protein was immobilized to the surface of the CM5 chip and only one k_{on} and k_{off} rate could be discerned on the sensorgrams, these observations suggest that, at physiological concentrations, the stoichiometry is 1:1, with monomeric VV-35kDa binding monomeric MCP-1.

Table 1. Kinetic and affinity binding parameters for MCP-1 mutants binding VV-35kDa

Mutant	k_{on}, $\times 10^7$ $M^{-1}{\cdot}s^{-1}$*	k_{off}, $\times 10^{-2}$ s^{-1}*	K_D, nM†
wtMCP-1	5.59 ± 2.0	1.90 ± 0.69	0.339
Met-MCP-1	4.34 ± 1.39	1.06 ± 0.26	0.243
7ND	9.65 ± 3.76	1.38 ± 1.15	0.143
3-7A	5.87 ± 5.93	0.73 ± 0.07	0.124
D3A	3.52 ± 1.64	0.81 ± 0.76	0.231
I5P	4.98 ± 1.39	1.58 ± 0.44	0.317
P8A	7.06 ± 3.42	2.57 ± 1.71	0.364
V9E	4.12 ± 1.36	0.59 ± 0.17	0.143
V9A + T10A	4.35 ± 2.72	1.02 ± 0.34	0.234
T10E	2.52 ± 0.65	4.77 ± 0.90	1.893
Y13A	**4.07 ± 0.72**	**12.97 ± 1.45**	**3.189**
N14A	5.31 ± 1.75	2.29 ± 1.01	0.431
F15A	3.73 ± 1.29	1.11 ± 0.46	0.296
N17A	3.30 ± 0.45	1.82 ± 0.26	0.551
R18A	**1.12 ± 0.38**	**13.43 ± 2.32**	**12.044**
K19A	**2.60 ± 0.81**	**4.13 ± 1.29**	**1.589**
Q23A	2.99 ± 0.86	1.41 ± 0.05	0.472
R24A	**1.07 ± 0.36**	**6.42 ± 2.18**	**5.986**
R24E	ndb	ndb	ndb
R24Q	1.86 ± 0.011	11.05 ± 1.23	5.943
S27A	3.39 ± 0.45	0.78 ± 0.12	0.230
Y28A	3.08 ± 1.77	1.43 ± 0.67	0.465
R29A	2.49 ± 0.60	0.99 ± 0.22	0.399
R30A	3.35 ± 0.81	1.57 ± 0.19	0.469
T32A	3.18 ± 0.36	1.71 ± 0.05	0.536
S33A	5.00 ± 0.51	2.38 ± 0.14	0.476
S34A	4.15 ± 0.85	1.12 ± 0.36	0.270
34P35	8.33 ± 2.92	13.05 ± 4.51	1.565
K35A	5.08 ± 2.29	1.73 ± 0.36	0.340
K35E	5.94 ± 0.18	3.64 ± 1.50	0.613
P37A	5.79 ± 1.49	3.26 ± 0.91	0.564
K38A	**3.72 ± 1.24**	**3.66 ± 0.71**	**0.986**
K38E	1.27 ± 0.18	3.91 ± 0.37	3.071
K35E/K38E	1.64 ± 0.68	7.27 ± 3.81	4.438
E39A	4.70 ± 0.80	1.74 ± 0.65	0.371
K44A	8.34 ± 2.50	1.78 ± 0.55	0.214
I46A	5.61 ± 2.10	1.60 ± 0.80	0.284
K49A	**1.11 ± 0.14**	**0.17 ± 0.04**	**0.150**
E50A	3.14 ± 0.78	1.18 ± 0.28	0.377
K56A	3.29 ± 0.22	1.43 ± 0.14	0.434
Q57A	3.62 ± 0.36	1.24 ± 0.75	0.342
K58A	5.41 ± 1.20	2.79 ± 1.59	0.516
H66A	5.37 ± 2.73	2.23 ± 1.48	0.415
K69A	5.07 ± 2.58	2.32 ± 0.98	0.457

ndb, no detectable binding. Boldface indicates Ala mutant that affects binding to VV-35kDa compared with wtMCP-1.

*Values shown are the mean ± SD from analysis of three replicate sets.

†K_D was determined using the relationship between k_{on} and k_{off} ($K_D = k_{off}/k_{on}$).

To further evaluate whether VV-35kDa interacts with MCP-1 with 1:1 stoichiometry, we used the noncovalently immobilized VV-35kDa-Fc fusion protein to monitor the precise mass of the VV-35kDa-Fc fusion protein immobilized at the surface. From the ratio of the molecular masses of VV-35kDa-Fc and MCP-1, R_{max} and the amount of VV-35kDa-Fc immobilized, we calculated that one molecule of dimeric (divalent) VV-35kDa-Fc protein interacts with two molecules of MCP-1. To determine whether the observed stoichiometry resulted from one dimeric MCP-1 molecule or two monomeric MCP-1 molecules, we again used the monomeric P8A ($k_{on} = 1.38 \times 10^7$ $M^{-1}{\cdot}s^{-1}$; $k_{off} = 0.0157$ s^{-1}; $K_D = 1.14$ nM), and demonstrated that wtMCP-1 and P8A saturate at identical R_{max} levels of ≈30 RU (not shown).

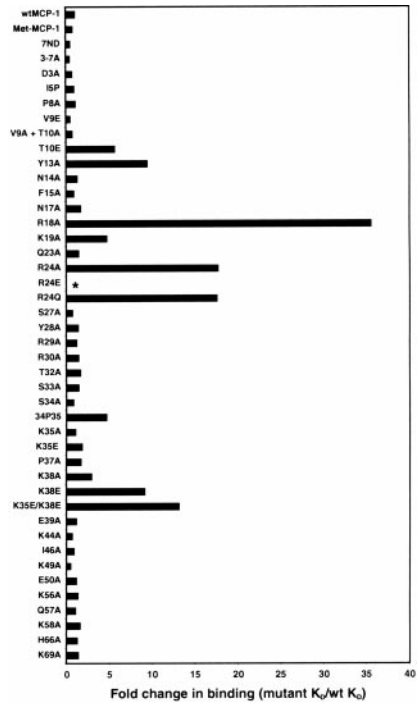

Fig. 2. Fold changes in equilibrium dissociation affinity constants for mutants relative to wtMCP-1. Fold changes in binding were determined from the ratio of the K_D for mutant MCP-1 compared with wtMCP-1 binding to VV-35kDa. An asterisk indicates that this mutant displayed no detectable binding

Together, these observations demonstrate that, at these concentrations, MCP-1 binds VV-35kDa as a 1:1 complex formed from 1 monomeric unit of VV-35kDa and 1 monomeric unit of MCP-1.

N-Terminal Residues of MCP-1 Are Not Critical for Binding to VV-35kDa. Structure/function studies of several chemokines, including MCP-1, have demonstrated that the N-terminal region before the first cysteine is a key determinant for receptor signaling and, in some cases, contributes to the binding affinity (6, 8, 9, 12, 14, 15, 19, 22, 48). To probe the role of the N terminus of MCP-1 in binding VV-35kDa, kinetic and affinity parameters were determined for a series of single and multiple point mutants and for a deletion mutant. D3A, N6A, and a triple mutant (D3A + I5A + N6A or 3-7A MCP-1) had no significant effect on the rate constants or binding affinity (Table 1, Fig. 2). We also tested a mutant containing a proline substitution for isoleucine at position 5 (I5P), which would be expected to disrupt the putative 3^{10} helix observed in the crystal structure of MCP-1 (49), but found no change in binding affinity. A double mutation of V9 and T10 to alanine (V9A/T10A) also had no effect on binding to VV-35kDa (Table 1), although mutation of T10 to Glu (T10E) produced a 6-fold reduction in affinity, suggesting that the residue at position 10 to may be positioned close to a complementary region on VV-35kDa that is negatively charged. Extension of MCP-1 by adding methionine at the N terminus (Met-MCP-1) had no effect on binding VV-35kDa, although this mutation does affect MCP-1 binding to CCR2b. Finally, binding of 7ND, a 7-aa N-terminal deletion mutant (6, 12, 13, 50), demonstrated that the presence of an intact N terminus was not critical for binding VV-35kDa.

VV-35kDa Contacts Many of the Same Residues of MCP-1 That Contribute to CCR2b Binding. It was previously shown that two clusters of primarily basic residues (R24, K35, K38, K49, and Y13) make

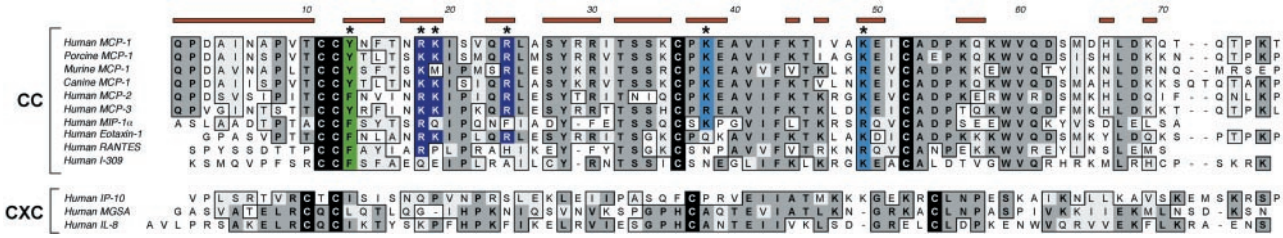

Fig. 3. Alignment of CC-chemokines. Human MCP-1 aligned with a set of representative CC-chemokines. The red line over the MCP-1 sequence shows the MCP-1 residues that were tested for binding against VV-35kDa. Residues in black illustrate the conserved cysteines. MCP-1 residues involved in binding VV-35kDa are shown with asterisks above the residues and are also shown in color to illustrate their conservation amongst CC-chemokines. Residues are colored in the following manner: light blue represents basic residues that affected binding by a factor less than 5; purple represents basic residues that affected binding greater than 5-fold; green represents aromatic residues that affected binding. Murine MCP-1 is shown only up to residue 76.

the largest contributions to the interaction between MCP-1 and CCR2b (15- to 100-fold; ref. 6). Using the same panel of mutants, we investigated whether VV-35kDa shares the same contact points on MCP-1 as does CCR2b.

Table 1 and Fig. 2 summarize the results for these and other MCP-1 mutants. Of all of the alanine mutants, R18A produced the largest change (35-fold) in the binding affinity to VV-35kDa. Mutation of the adjacent residue K19 to alanine reduced the binding by ≈4.5-fold. These significant reductions in affinity contrast with the binding to CCR2b where these mutations made only a modest 2- to 3-fold change. On the other hand, these two residues appear to be critical for the interaction of MCP-1 with glycosaminoglycans (E.K.L. and T.M.H., unpublished results). The reduction in affinity because of these mutations is a result of a moderate decrease in the association rate and a significant increase in the dissociation rate (Table 1, Fig. 1*C*). Interestingly, R18 is highly conserved as a basic residue (lysine or arginine) in many CC-chemokines (Fig. 3). This conservation is also true of K19, although to a lesser extent. Thus, these basic residues may be important in poxvirus CBP interactions with other CC-chemokines, contributing to the promiscuity of binding partners.

Arginine at position 24 is also highly conserved among MCPs and resides within a 3^{10} helix present in every known CC-chemokine structure (6). Mutation of R24 to alanine (R24A) produced the second largest reduction (17-fold) in the interaction with VV-35kDa (Table 1, Fig. 1*D*), similar to the effect that R24A had on binding CCR2b (35-fold). We also examined the effect of substituting R24 with glutamine (R24Q), a polar but uncharged residue, and found no difference in binding affinity compared with R24A (Table 1, Fig. 2). To assess the role of electrostatics at this position, we substituted R24 with glutamic acid (R24E). This mutant virtually abolished binding, suggesting that R24 forms a critical interaction with a negatively charged region of VV-35kDa, as was observed for CCR2b.

Additional basic residues that were important for CCR2b binding include K49, K35, and K38 (Fig. 4*B*). K49A had little effect on binding affinity to VV-35kDa; in fact it increased the affinity slightly in contrast to the 14- to 15-fold reduction observed for CCR2b binding. One possible explanation for this result is that the interaction between MCP-1's K49 and VV-35kDa is destabilizing, but contributes to specificity in the complex similar to buried polar groups observed in other complexes such as coiled coils (51, 52). K38A displayed a minimal 3-fold reduction in affinity (Table 1, Fig. 2), whereas mutation to glutamic acid resulted in a 9-fold reduction, similar to what was observed for CCR2b. Thus, this basic residue may also confer specificity to the formation of the complex while contributing little to affinity.

Apart from these basic residues, Y13 was the only other residue identified as a contact residue for VV-35kDa from an extensive panel of mutants. Previously, Y13A caused the single largest decrease in binding to CCR2b and was also found to be necessary for CCR2b signaling (6, 8). For VV-35kDa, the binding affinity of Y13A was reduced by ≈10-fold, which is the third largest change in affinity of all of the alanine mutants tested. This residue is also conserved as a phenylalanine, tyrosine, or leucine among many CC-chemokines (Fig. 3), suggesting that aromaticity and/or hydrophobicity at this position may be important for recognition by VV-35kDa.

As in the screen against CCR2b (6), the only other significant effect was observed for 34P35, a mutant containing a proline

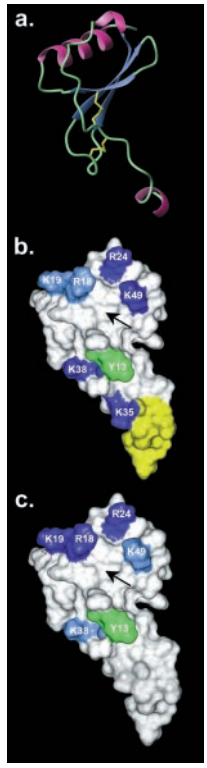

Fig. 4. Comparison of the binding determinants of MCP-1 for CCR2b and VV-35kDa. (*a*) Ribbon diagram of the backbone structure of a monomeric subunit of MCP-1 extracted from the x-ray structure (49). The figure was generated by using MOLMOL (56). Panels *b* and *c* were generated in INSIGHTII (San Diego, CA) by using the NMR structure (57) and shows van der Waal surface representations of MCP-1 with residues that are important for binding to (*b*) CCR2b and (*c*) VV-35kDa protein, colored in the following manner: light blue represents basic residues that affected binding by a factor less than 5; purple represents basic residues that affected binding greater than 5-fold; green represents aromatic residues that affected binding; yellow represents the N terminus involved in CCR2b signaling. The hydrophobic groove identified as an interaction site by NMR titration of a peptide from the N terminus of CCR2 is indicated with an arrow.

insertion between residues 34 and 35. We found that 34P35 reduced the binding affinity by 4.6-fold. However, the effect is likely due to a structural perturbation that alters the relative orientation of key residues in the 30s loop (e.g., K38) and the N-loop (e.g., Y13) to which it is structurally coupled via the first disulfide. Indeed, it was previously shown (6) that this mutation eliminated the ability of MCP-1 to dimerize, presumably because of structural changes propagated to residues that stabilize the dimer (e.g., Y13).

Discussion

Given the role of CC-chemokines as key mediators of the immune response during normal and chronic inflammatory situations, understanding the interaction between a soluble, secreted viral CC-chemokine binding protein and CC-chemokines provides useful insights into structural aspects of viral immunology as well as chemokine biology. In addition to contributing to the understanding of the functional epitopes of chemokines, such studies should also help facilitate the rational design of chemokine receptor antagonists. In the present study, SPR (BIAcore) was used to identify specific residues of human MCP-1 that contribute to the interaction with VV-35kDa. We determined the contribution of individual amino acids by monitoring the real-time binding of wild-type and mutant MCP-1 to immobilized VV-35kDa. From a detailed kinetic analysis of the data, we were able to extract information regarding the speed, stability, specificity, and stoichiometry of the VV-35kDa/MCP-1 complex.

This study confirms that wtMCP-1 binds VV-35kDa with high affinity (K_D = 340 pM, $\Delta G = -12.9$ kcal·mol^{-1}) as a result of very fast association rates and reasonably slow dissociation rates. As a functional inhibitor of chemokines, the binding parameters described are well within the realm to competitively block the interaction of MCP-1 to its receptor CCR2b, whose reported K_D ranges from 35 pM to 440 pM (6, 53, 54). Control experiments of wtMCP-1 binding the VV-35kDa-Fc fusion protein demonstrated a K_D of 1.29 nM. In addition to validating values determined for VV-35kDa using SPR, the Fc-fusion protein permitted comparison of SPR technology to other methods used in other studies. For instance, the use of a scintillation proximity assay demonstrated that human MCP-1 binds the VV-35kDa-Fc protein with a K_D of 15.1 nM (29), whereas plate-binding assays showed that murine MCP-1 could bind an Fc-fusion construct of the highly related CPV-p35 protein with a K_D of 83 pM (28). We conclude that SPR technology offers comparable binding constants and that no artifacts were introduced as a result of the coupling chemistry.

Alcamí *et al.* (29) suggested that the binding stoichiometry of VV-35kDa with MCP-1 is 1:2; but in our hands, using both the monomeric VV-35kDa protein and the dimeric VV-35kDa-Fc fusion protein, the stoichiometry is 1:1 at physiological concentrations of MCP-1. Furthermore, the association and dissociation profiles show evidence for only one affinity class of binding sites. Finally, P8A, a mutant that does not dimerize, had almost identical binding and saturation parameters as wtMCP-1. Although these observations do not rule out the possibility that the monomeric VV-35kDa protein can interact with a dimer of MCP-1 in solution at higher concentrations of MCP-1, we predict that *in vivo* monomeric VV-35kDa interacts with monomeric MCP-1, supporting the idea that VV-35kDa has evolved to recognize the biologically relevant form of CC-chemokines.

The amino acid sequence and length of the N-terminal region preceding the dicysteine motif of CC-chemokines is highly variable (Fig. 3) and likely imparts specificity in signaling through cognate receptors. Using mutants of MCP-1 that were altered within the first 7 N-terminal amino acids, we showed that this region does not participate in binding of MCP-1 to VV-35kDa. Despite observations that the N-terminal regions of some chemokines are necessary for binding to receptors (5, 6, 9, 14, 20, 22, 55), the absence of a contribution of MCP-1's N terminus in binding VV-35kDa is consistent with our hypothesis that the viral protein does not contact regions of high disparity but recognizes epitopes that are relatively conserved amongst the CC-chemokines.

Although mutation of most residues in MCP-1 had little or no effect on binding affinity, significant effects were observed for three residues within the so-called "N-loop" (Y13, R18, and K19) and one residue, R24, within the 3^{10} helix. The importance of Y13 as a residue involved in binding VV-35kDa provides additional evidence in favor of the 1:1 stoichiometry; the use of Y13 by VV-35kDa would likely obstruct MCP-1 dimer formation because Y13 is sequestered in the interface of the MCP-1 dimer. Mutation of K38 and K49 to alanine produced minor effects on binding affinity but may contribute to specificity of the complex. Analogous to the binding surface mapped by mutagenesis for CCR2b (Fig. 4*B*), these residues define two discontinuous, largely basic, regions of the chemokine surface separated by a hydrophobic groove (Fig. 4*C*).

Supporting the notion that basic residues on CC-chemokines play a role in binding VV-35kDa, the recent crystal structure of the related CPV CC-chemokine binding protein revealed a highly negatively charged surface that could complement the constellation of basic residues identified on MCP-1 (31). However, analysis of the energetic contribution of the basic residues fails to fully account for the free energy change for the interaction of wtMCP-1 with VV-35kDa ($\Delta G = -12.9$ kcal·mol^{-1}), suggesting that additional epitopes contribute to CC-chemokine binding. For example, interactions with backbone atoms could be involved, but cannot be identified by mutagenesis. Residues within the hydrophobic groove of MCP-1 (Fig. 4 *B* and *C*) could also contribute to the interaction; these residues were not mutated because of the possibility of structural perturbation. However, a peptide derived from the N terminus of CCR2b was shown to interact with the groove (6) (L. Mizoue, unpublished results). Because VV-35kDa is large in comparison with MCP-1 and makes contact with residues that flank the groove, it is possible that the viral protein also contacts the intervening hydrophobic groove where CCR2b's N terminus purportedly binds, thereby forming a continuous interaction surface. In sum, VV-35kDa not only binds to the same molecular face on MCP-1 that is used for CCR2b, but also interacts with many of the same residues that constitute recognition hotspots for the host receptor (Fig. 4 *B* and *C*). The observation that similar binding epitopes are used for recognition of both VV-35kDa and CCR2b provides a structural basis for the ability of VV-35kDa to occlude the binding of MCP-1 with its host receptor.

Similar arguments can be extended to the interaction of VV-35kDa with other CC-chemokines to explain the broad-spectrum inhibition. For example, RANTES (regulated upon activation, normal T cell expressed and secreted) requires R17 (MCP-1's R18 equivalent) to bind CCR1, F12 (MCP-1's Y13 equivalent) to bind CCR3, and both F12 and I15 to bind CCR5 (9). Likewise, macrophage inflammatory protein-1β (MIP-1β) requires F13 (MCP-1's Y13 equivalent) to bind CCR5 (46), and we predict that the corresponding residue in MIP-1α will also be necessary. We also speculate that R18 in MIP-1α and MIP-1β will be critical for binding VV-35kDa, similar to R18 of MCP-1. Finally, several groups have also shown interactions between other chemokines and N-terminal receptor peptides (7, 11, 15, 18), suggesting that additional residues on the same face of chemokines may constitute a common recognition feature of chemokines by chemokine receptors. Interaction with this common binding region by VV-35kDa suggests how VV-35kDa could obstruct other CC-chemokines from binding their receptors.

The present study supports a model whereby VV-35kDa interacts over a large surface area that includes the N-loop, the

downstream 3^{10} helix, and possibly a region spanning the hydrophobic groove of MCP-1 (Fig. 4*C*). These are significant contact points that are not only structurally conserved amongst CC-chemokines (Fig. 3), but are also necessary to initiate binding to their GPCRs, the first step in receptor activation. Other studies (28, 29) and our own data (unpublished) involving the kinetic analysis of VV-35kDa with other CC-chemokines help to extend some of the predicted requirements that govern the specificity of the VV-35kDa interaction with CC-chemokines. For instance, relatively acidic chemokines (e.g., MIP-1α) continue to have a high affinity interaction, demonstrating that overall pI may have little role in regulating the recognition by VV-35kDa. On the other hand, the CC-chemokine I-309 has a relatively low affinity interaction with VV-35kDa (29) and may be due to the lack of basic residues at the corresponding positions to MCP-1's residues at positions 18, 19, 24, and 38 (Fig. 3) although the extra disulfide bond in I-309 may play a role in altering its structure in a manner that might affect binding. CXC-chemokines are basic proteins and fold similarly to CC-chemokines yet do not bind VV-35kDa with any appreciable affinity. A plausible explanation for this very low or absent binding to CXC-chemokines may be that the residues identified here are not typically found in the corresponding position among CXC-chemokines although the formal possibility exists that the CXC motif itself may be one of the distinguishing features for recognition by VV-35kDa. Nonetheless, the present results suggest that the VV-35kDa has recapitulated a similar binding surface to that provided by CC-chemokine receptors for binding CC-chemokines.

In summary, despite the amino acid sequence diversity among CC-chemokines, VV-35kDa and members of the T1/35-kDa family of CC-chemokine inhibitors possess the unique ability to bind many CC-chemokines with high affinity. The results presented here represent one of the most extensive studies examining a viroceptor's structural interaction with a host ligand and help explain both the ability of VV-35kDa to block CC-chemokines from their GPCRs and its capacity for broad-spectrum recognition of CC-chemokines. Future studies involving the analysis of site-directed mutants of VV-35kDa and solution of crystal structures of complexes should help further elucidate the molecular details of this broad-spectrum interaction and define the complete energetic parameters that contribute to binding. The discovery that poxviruses produce a novel set of proteins to broadly disrupt CC-chemokines underscores the importance of CC-chemokines during viral infection (23, 24). Lessons from this family of viral chemokine inhibitors highlight important structural features of chemokine/chemokine receptor interactions and point toward strategies to rationally develop antagonists of chemokine function.

We thank Dr. Colin Macaulay, Dr. John Barrett, Dr. Kara Herlihy, and Dr. Piers Nash for useful discussions. B.T.S. was supported by the Ontario Graduate Scholarship for Science and Technology provided by the Government of Ontario and the University of Western Ontario. G.M. is a Canadian Institutes of Health Research Senior Scientist. T.M.H. was supported by a grant from the National Institutes of Health and the American Heart Association. This manuscript is dedicated to the memory of Bruce Semper, a friend and mentor of B.T.S.

1. Rollins, B. J. (1997) *Blood* **90,** 909–928.
2. Baggiolini, M. (1998) *Nature (London)* **392,** 565–568.
3. Rossi, D. & Zlotnik, A. (2000) *Annu. Rev. Immunol.* **18,** 217–242.
4. Beall, C. J., Mahanjan, S., Kuhn, D. & Kolattukudy, P. (1996) *Biochem. J.* **313,** 633–640.
5. Gong, J. H. & Clark-Lewis, I. (1995) *J. Exp. Med.* **181,** 631–640.
6. Hemmerich, S., Paavola, C., Bloom, A., Bhakta, S., Freedman, R., Grunberger, D., Krstenansky, J., Lee, S., McCarley, D., Mulkins, M., *et al*. (1999) *Biochemistry* **38,** 13013–13025.
7. Mizoue, L., Bazan, J. F., Johnson, E. C. & Handel, T. M. (1999) *Biochemistry* **38,** 1402–1414.
8. Jarnagin, K., Grunberger, D., Mulkins, M., Wong, B., Hemmerich, S., Paavola, C., Bloom, A., Bhakta, S., Diehl, F., Freedman, R., *et al*. (1999) *Biochemistry* **38,** 16167–16177.
9. Pakianathan, D. R., Kuta, E. G., Artis, D. R., Skelton, N. J. & Hebert, C. A. (1997) *Biochemistry* **36,** 9642–9648.
10. Williams, G., Borkakoti, N., Bottomley, G. A., Cowan, I., Fallowfield, A. G., Jones, P. S., Kirtland, S. J., Price, G. J. & Price, L. (1996) *J. Biol. Chem.* **271,** 9579–9586.
11. Skelton, N. J., Quan, C., Reilly, D. & Lowman, H. (1999) *Structure* **7,** 157–168.
12. Zhang, Y. J., Rutledge, B. J. & Rollins, B. J. (1994) *J. Biol. Chem.* **269,** 15918–15924.
13. Zhang, Y., Ernst, C. A. & Rollins, B. J. (1996) *Methods* **10,** 93–103.
14. Mayer, M. R. & Stone, M. J. (2001) *J. Biol. Chem.* **276,** 13911–13916.
15. Mayer, K. L. & Stone, M. J. (2000) *Biochemistry* **39,** 8382–8395.
16. Clark-Lewis, I., Kim, K. S., Rajarathnam, K., Gong, J. H., Dewald, B., Moser, B., Baggiolini, M. & Sykes, B. D. (1995) *J. Leukocyte Biol.* **57,** 703–711.
17. Gayle, R. B., Sleath, P. R., Srinivason, S., Birks, C. W., Weerawarna, K. S., Cerretti, D. P., Kozlosky, C. J., Nelson, N., Vanden Bos, T. & Beckmann, M. P. (1993) *J. Biol. Chem.* **268,** 7283–7289.
18. Clubb, R. T., Omichinski, J. G., Clore, G. M. & Gronenborn, A. M. (1994) *FEBS Lett.* **338,** 93–97.
19. Crump, M. P., Gong, J. H., Loetscher, P., Rajarathnam, K., Amara, A., Arenzana-Seisdedos, F., Virelizier, J. L., Baggiolini, M., Sykes, B. D. & Clark-Lewis, I. (1997) *EMBO J.* **16,** 6996–7007.
20. Gong, J.-H., Uguccioni, M., Dewald, B., Baggiolini, M. & Clark-Lewis, I. (1996) *J. Biol. Chem.* **271,** 10521–10527.
21. Hebert, C. A., Vitangcol, R. V. & Baker, J. B. (1991) *J. Biol. Chem.* **266,** 18989–18994.
22. Clark-Lewis, I., Schumacher, C., Baggiolini, M. & Moser, B. (1991) *J. Biol. Chem.* **266,** 23128–23134.
23. Lusso, P. (2000) *Virology* **273,** 228–240.
24. McFadden, G. & Murphy, P. M. (2000) *Curr. Opin. Microbiol.* **3,** 371–378.
25. Mahalingam, S., Clark, K., Matthaei, K. I. & Foster, P. S. (2001) *Bioessays* **23,** 428–435.
26. Lalani, A. S., Barrett, J. & McFadden, G. (2000) *Immunol. Today* **21,** 100–106.
27. Graham, K. A., Lalani, A. S., Macen, J. L., Ness, T. L., Barry, M., Liu, L.-Y., Lucas, A., Clark-Lewis, I., Moyer, R. W. & McFadden, G. (1997) *Virology* **229,** 12–24.
28. Smith, C. A., Smith, T. D., Smolak, P. J., Friend, D., Hagen, H., Gerhart, M., Park, L., Pickup, D. J., Torrance, D., Mohler, K., Schooley, K. & Goodwin, R. G. (1997) *Virology* **236,** 316–327.
29. Alcamí, A., Symons, J. A., Collins, P. D., Williams, T. J. & Smith, G. L. (1998) *J. Immunol.* **160,** 624–633.
30. Smith, V. P. & Alcamí, A. (2000) *J. Virol.* **74,** 8460–8471.
31. Carfi, A., Smith, C. A., Smolak, P. J., McGrew, J. & Wiley, D. C. (1999) *Proc. Natl. Acad. Sci. USA* **96,** 12379–12383.
32. Paavola, C. D., Hemmerich, S., Grunberger, D., Polsky, I., Bloom, A., Freedman, R., Mulkins, M., Bhakta, S., McCarley, D., Wiesent, L., *et al*. (1998) *J. Biol. Chem.* **273,** 33157–33165.
33. Johnsson, B., Lofas, S. & Lindquist, G. (1991) *Anal. Biochem.* **198,** 268–277.
34. Myszka, D. G. (1999) *J. Mol. Recognit.* **12,** 279–284.
35. Morton, T. A. & Myszka, D. G. (1998) *Methods Enzymol.* **295,** 268–294.
36. Chung, C., Cooke, R. M., Proudfoot, A. E. I. & Wells, T. N. C. (1995) *Biochemistry* **34,** 9307–9314.
37. Graham, G. J., MacKenzie, J., Lowe, S., Tsang, M. L.-S., Weatherbee, J. A., Issacson, A., Medicherla, J., Fang, F., Wilkinson, P. C. & Pragnell, I. B. (1994) *J. Biol. Chem.* **269,** 4974–4978.
38. Schnitzel, W., Monschein, U. & Besemer, J. (1994) *J. Leukocyte Biol.* **55,** 763–770.
39. Crump, M. P., Rajarathnam, K., Kim, K. S., Clark-Lewis, I. & Sykes, B. D. (1998) *J. Biol. Chem.* **273,** 22471–22479.
40. LiWang, A. C., Cao, J., Zheng, H., Lu, Z., Peiper, S. C. & LiWang, P. J. (1999) *Biochemistry* **38,** 442–453.
41. Rajarathnam, K., Kay, C. M., Dewald, B., Wolf, M., Baggiolini, M., Clark-Lewis, I. & Sykes, B. D. (1997) *J. Biol. Chem.* **272,** 1725–1729.
42. Rajarathnam, K., Li, Y., Rohrer, T. & Gentz, R. (2001) *J. Biol. Chem.* **276,** 4909–4916.
43. Sticht, H., Escher, S. E., Schweimer, K., Forssmann, W.-G., Rosch, P. & Adermann, K. (1999) *Biochemistry* **38,** 5995–6002.
44. Kim, K. S., Rajarathnam, K., Clark-Lewis, I. & Sykes, B. D. (1996) *FEBS Lett.* **395,** 277–282.
45. Paolini, J. F., Willard, D., Consler, T., Luther, M. & Krangel, M. S. (1994) *J. Immunol.* **153,** 2704–2717.
46. Laurence, J. S., Blanpain, C., Burgner, J. W., Parmentier, M. & LiWang, P. J. (2000) *Biochemistry* **39,** 3401–3409.
47. Rajarathnam, K., Sykes, B. D., Kay, C. M., Dewald, B., Geiser, T., Baggiolini, M. & Clark-Lewis, I. (1994) *Science* **264,** 90–92.
48. Elisseeva, E. L., Slupsky, C. M., Crump, M. P., Clark-Lewis, I. & Sykes, B. D. (2000) *J. Biol. Chem.* **275,** 26799–26805.
49. Lubkowski, J., Bujacz, G., Boque, L., Domaille, P. J., Handel, T. M. & Wlodawer, A. (1997) *Nat. Struct. Biol.* **4,** 64–69.
50. Zhang, Y. & Rollins, B. J. (1995) *Mol. Cell. Biol.* **15,** 4851–4855.
51. Hendsch, Z. S. & Tidor, B. (1999) *Protein Sci.* **8,** 1381–1392.
52. Lumb, K. J. & Kim, P. S. (1998) *Biochemistry* **34,** 8642–8648.
53. Han, K. H., Green, S. R., Tangirala, R. K., Tanaka, S. & Quehenberger, O. (1999) *J. Biol. Chem.* **274,** 32055–32062.
54. Myers, S. J., Wong, L. M. & Charo, I. F. (1995) *J. Biol. Chem.* **270,** 5786–5792.
55. Loetscher, P., Gong, J. H., Dewald, B., Baggiolini, M. & Clark-Lewis, I. (1998) *J. Biol. Chem.* **273,** 22279–22283.
56. Koradi, R., Billeter, M. & Wüthrich, K. (1996) *J. Mol. Graphics* **14,** 52–55.
57. Handel, T. M. & Domaille, P. J. (1996) *Biochemistry* **35,** 6569–6584.